

COMPARISON OF ORBIT THEORIES FOR SEPARATED SECTORED CYCLOTRONS

A. Jain and A.S. Divatia

Variable Energy Cyclotron Project, Bhabha Atomic Research Centre, Trombay, Bombay, India.

Abstract

For the design of "flared" sectors in medium and high energy separated sector cyclotrons, hard edge expressions obtained by the following two methods can be used to calculate the betatron oscillation frequencies directly from the sector drawings 1) expressions obtained using a hard edge Fourier analysis approach, 2) expressions obtained by the method of multiplication of matrices. A comparison is made of the two sets of expressions.

1. Introduction

For designing the sectors of a medium or high energy separated sector cyclotron, it is convenient to have hard edge expressions which will relate the betatron frequencies ν_z and ν_r and the time period τ directly to the sector drawings. To obtain these expressions two alternative methods may be used: 1) a "hard edge" Fourier analysis approach, described earlier^{1,2} and 2) the "matrix multiplication" approach³. These are summarized below:

1.1 Hardedge Fourier Analysis Approach

To obtain the hardedge expressions for the betatron frequencies when 1) the sector entry and exit spiral angles ϵ_1 and ϵ_2 are unequal, and 2) the hill angle η_0 , the hill field B_H and valley field B_V are all functions of the radius, we may begin with the analytical expressions for the betatron frequencies

$$\nu_z^2 = -\mu' + F^2 + \sum_i \frac{a'n^2 + b'n^2}{n^2} \quad (1)$$

$$\nu_r^2 = 1 + \mu' + \dots \quad (2)$$

derived by Smith & Garren⁴, Verster and Hagedoorn⁵). We reduce these expressions to the equivalent hardedge set.

In the hardedge approximation, the average field B_0 over the circle of radius ρ_0 is

$$B_0 = \frac{N}{2\pi} [B_H \eta_0 + B_V \xi_0] \quad (3)$$

where N =number of sectors, and ξ_0 the valley angle.

When η_0, ξ_0, B_H and B_V are all functions of the radius, the total field index $\mu'T$ is obtained by differentiating Eq.(3) in all the functions.

$$\mu'T = \frac{\rho_0}{B_0} \frac{dB_0}{d\rho_0} = (\tan \epsilon_2 - \tan \epsilon_1)/R_4 + \frac{N\eta_0 B_H \eta_H}{2\pi B_0} + \frac{B_V}{B_0} (1 - \frac{N\eta_0}{2\pi}) \frac{B_V \nu_V}{B_0} \quad (4)$$

where $R_4 = \eta_0 [1 + 2\pi B_V / \eta_0 N (B_H - B_V)]$ and we have made use of the relation

$$\frac{d\eta_0}{d\rho_0} - \frac{1}{\rho_0} (\tan \epsilon_2 - \tan \epsilon_1) = 0 \quad (5)$$

η_H is the hill field index $\frac{\rho_0}{B_H} \frac{dB_H}{d\rho_0}$ and ν_V the valley field index $\frac{\rho_0}{B_V} \frac{dB_V}{d\rho_0}$ for flat sectors $\eta_H = \nu_V = 0$.

The radial derivatives of the Fourier coefficients a_n' and b_n' required in Eq.1 can also be obtained directly from the sector drawings. With reference to Fig.1, we Fourier analyse a step wave in the interval $0 < \theta < 2\pi$ by dividing the interval into regions a_1, a_2, a_3, a_4, a_5 and a_6 (though the case of $N=3$ sectors is shown in Fig.1, the results can be generalized to any N). Since the n th Fourier co-efficients are given by

$$p_n = \frac{1}{\pi} \int_0^{2\pi} B(\theta) \cos n\theta d\theta, \quad q_n = \frac{1}{\pi} \int_0^{2\pi} B(\theta) \sin n\theta d\theta \quad (6)$$

we get, evaluating the integrals,

$$p_n(\rho_0) = \frac{1}{\pi n} \left[(B_V - B_H) (\sin na_1 + \sin na_3 + \sin na_5) + (B_H - B_V) (\sin na_2 + \sin na_4 + \sin na_6) \right] \quad (7)$$

At radius $\rho_0 + \Delta\rho_0$, due to the spiralling, the entry and exit sector edges will be displaced by $\Delta\theta_1$ and $\Delta\theta_2$ respectively shown by the dotted step wave in Fig.1. Changing the intervals $a_1 \rightarrow a_1 + \Delta\theta_1$ etc. and again evaluating the integrals

$$p_n(\rho_0 + \Delta\rho_0) = \frac{1}{\pi n} \left\{ (B_V - B_H) [\sin n(a_1 + \Delta\theta_1) + \dots] + (B_H - B_V) [\sin n(a_2 + \Delta\theta_2) + \dots] \right\} \quad (8)$$

Thus putting $a_3 = a_1 + 2\pi/N$ etc., and taking limits

$$p_n(\rho_0 + \Delta\rho_0) - p_n(\rho_0) = \frac{N}{\pi} (B_H - B_V) [\Delta\theta_2 \cos n(\beta_0 + \eta_0) - \Delta\theta_1 \cos n\beta_0] \quad (9)$$

where β_0 may be any arbitrary angle between 0 and a_1 and η_0 the hill angle. Since

$$a_n' = \frac{\rho_0}{B_0} \frac{dp_n}{d\rho_0} \quad \text{and} \quad \tan \epsilon = \rho_0 \frac{d\theta}{d\rho_0}$$

taking limits in Eq.9

$$a'_n = \frac{Nf_1}{\pi} [\tan \epsilon_2 \cos n(\beta_0 + \eta_0) - \tan \epsilon_1 \cos n\beta_0] \quad \dots (10)$$

where $f_1 = (B_H - B_V)/B_0$, Similarly,

$$b'_n = \frac{Nf_1}{\pi} [\tan \epsilon_2 \sin n(\beta_0 + \eta_0) - \tan \epsilon_1 \sin n\beta_0] \quad \dots (11)$$

From Eq.10 and 11 for $n=N$,

$$a_N'^2 + b_N'^2 = \frac{N^2 f_1^2}{\pi^2} [\tan^2 \epsilon_1 + \tan^2 \epsilon_2 - 2 \cos N\eta_0 \tan \epsilon_1 \tan \epsilon_2] \quad (12)$$

If we include the effect of the higher harmonics $n=2N, 3N$ etc. then Fourier analysing as before and taking limits we get, simply

$$\sum_{n=N, 2N, \dots}^{\infty} \frac{a_n'^2 + b_n'^2}{n^2} = \frac{f_1^2}{\pi^2} [S_1 \tan^2 \epsilon_1 + S_2 \tan^2 \epsilon_2 - 2S_3 \tan \epsilon_1 \tan \epsilon_2] \quad (13)$$

where $S_1 = S_2 = \sum_r \frac{1}{K^2}$ and $S_3 = \sum_r \frac{1}{K^2} \cos NK\eta_0$

The expression for the Flutter can be obtained in a similar manner. Fourier analysing as before, from (7) etc.

$$F^2 = \frac{1}{2} \sum a_n'^2 + b_n'^2 = \frac{1 f_1^2}{\pi^2} (S_1 - S_3) \quad (14)$$

Substituting from (4), (13) and (14) in Eq. (1), the general hard-edge expression for ν_z becomes

$$\nu_z^2 = -(\tan \epsilon_2 - \tan \epsilon_1)/R_4 - \frac{B_H N \eta_0}{B_0 2\pi} \eta_0 - \left(1 - \frac{N\eta_0}{2\pi}\right) \frac{B_V}{B_0} n_V + F^2 [1 + (S_1 \tan^2 \epsilon_1 + S_2 \tan^2 \epsilon_2 - 2S_3 \tan \epsilon_1 \tan \epsilon_2) (S_1 - S_3)^{-1}] \quad (15)$$

We note that Eq.15 is exactly equivalent to Eq.1. It will be valid in so far as Eq.1 is valid. Eq.1 is found to give sufficiently reasonable agreement with orbit integration results. Thus Eq.15 will also be sufficiently accurate for initial design work. It is a general hard edge expression for ν_z in the following sense i) the entry and exit spiral angles ϵ_1 and ϵ_2 may be unequal, ii) the hill and valley magnets may have a field index n_H and n_V . For flat sectors $n_H = n_V = 0$, iii) Eq.15 is valid both for conventional single magnet cyclotrons and for separated sector cyclotrons. In the latter case, B_V is simply zero.

It is interesting to note that when $\epsilon_1 = \epsilon_2 = \epsilon$, Eq.(15) reduces to the well known expression $\nu_z^2 = -\mu' + F^2(1 + 2\tan^2 \epsilon)$

From Eqs.(2) and (4), the corresponding hard edge expression for ν_r , for arbitrary sector shapes, becomes

$$\nu_r^2 = 1 + (\tan \epsilon_2 - \tan \epsilon_1)/R_4 + \frac{B_H N \eta_0}{B_0 2\pi} \eta_0 + \frac{B_V}{B_0} \left(1 - \frac{N\eta_0}{2\pi}\right) n_V \quad (16)$$

1.2 Expressions by the multiplication of matrices

For flat, homogeneous field, separated sector cyclotrons, it is also possible to derive expressions for the betatron frequencies by the method of multiplication of matrices of field free sections and homogeneous field bending magnets. Then

$$\cos(\nu_{r,z} 2\pi/N) = \frac{1}{2} \text{Tr}(M_f, M_{mr,z})$$

where M_f is the matrix of the field free sector, and $M_{mr,z}$ the matrix of the magnet sector for r and z motion respectively.

This has been done by G. Schatz³⁾ and the result is

$$\begin{aligned} \cos(2\pi \nu_z/N) &= 1 + \frac{\pi}{N} [\tan \gamma_1 - \tan \gamma_2] + \sin \frac{\pi}{N} \cdot \\ &\cdot \sin \left(\frac{\pi}{N} - \frac{\alpha}{2}\right) [\tan \gamma_2 - \tan \gamma_1 - \frac{2\pi}{N} \tan \gamma_1 \tan \gamma_2] \cdot \\ &\cdot \sin \frac{\alpha-1}{2} \end{aligned} \quad (17)$$

$$\begin{aligned} \cos(2\pi \nu_r/N) &= \frac{1}{2} \left\{ \cos\left(\frac{2\pi}{N} - \gamma_1\right) \cdot \cos \gamma_1^{-1} - \right. \\ &[2 \sin \frac{\pi}{N} \cdot \sin\left(\frac{\pi}{N} - \frac{\alpha}{2}\right) \cdot (1 + \tan \gamma_1 \tan \gamma_2) \cdot \\ &\cdot \sin(2\pi/N - \gamma_1 - \gamma_2) \cdot \sin \frac{\alpha-1}{2} \cdot \cos(\gamma_1 - \gamma_2)^{-1}] \\ &\left. + \cos\left(2\frac{\pi}{N} + \gamma_2\right) \cos \gamma_2^{-1} \right\} \end{aligned} \quad (18)$$

where

$$\gamma_1 = (\pi/N - \alpha/2 + \epsilon_1), \quad \gamma_2 = (\epsilon_2 - \pi/N + \alpha/2)$$

and α and s in his notation correspond to the hill angle η_0 and radius ρ_0 in the present notation.

2. Comparison of the "Fourier" and "matrix" methods.

We now compare the two sets of hard edge expressions. Eqs.15 and 16, obtained by the Fourier method, and Eqs.17 and 18 obtained by the matrix multiplication method by applying them on the same sector shapes. Table 1 and Fig.2 show the sector parameters of an $E = 1/3 mc^2$, $N = 8$, flat field, separated sector electron cyclotron magnet.

The betatron frequencies obtained using the Fourier expressions Eq.15 and 16 and the matrix expressions 17 and 18 for the parameters of Table 1 are compared in Figs.3 and 4.

We note that the "Fourier" method gives values of the betatron frequencies lower than the "matrix" method.

Table 1 - Hardedge sector parameters for an N=3, separated sector electron cyclotron magnet

ρ_0	η_0	ϵ_1	ϵ_2
cms	...°	...°	...°
5.0	9.90	32.42	34.88
7.0	11.39	35.62	40.53
9.00	13.32	40.14	48.71
11.0	17.98	46.68	60.16

3. Soft Edge Expression for ν_z

Due to fringing field effects, a real cyclotron field will never be a "sharp hard-edge" but will be a "soft edge" field. A Fourier analysis of a "soft edge" field will give a relatively smaller amplitude of the higher harmonics than the corresponding hard edge. This is illustrated in Table 2 for a sector magnet with very large fringing fields.

Table 2 - Comparison of the successive harmonic amplitudes $C_n^2 = (p_n^2 + q_n^2)^{1/2}$ for the measured "soft edge" and equivalent hard edge fields for an N=3, sector magnet with large fringing fields.

K	n	C_n	C_n'
	harmonic	hard-edge	soft-edge
		Gauss	Gauss
1	8	81.90	84.79
2	16	50.54	16.83
3	24	14.18	2.62
4	32	12.35	3.56

Thus the hard edge Eq.15 is expected to overestimate the values of ν_z .

We note from Table 2 that the amplitude of the higher harmonics fall off rapidly compared to the fundamental. The effect of a higher harmonic already falls off as $1/K^2$ in Eq.15. Thus the net contribution of a higher harmonic falls off much faster than $1/K^2$.

It is sufficient to truncate the series in Eq.15 at a low value of K=2 or 3 consistent with the soft edge field. Eq.15 then becomes the relatively more accurate "soft edge" expression for ν_z .

A relative comparison of the hard edge Eq.15 (with $K = \infty$) and the soft edge Eq.15 (with K=2 and K=3) using the sector parameters²⁾ of an N=3, E=1/2 mc² electron cyclotron magnet is made in Fig.5. The experimental values of ν_z obtained by orbit integration in the measured field are also shown in the figure. As expected, because of the reasons mentioned earlier, K=∞ gives values of ν_z higher than the orbit integration results.

3.1 Flexibility of the Fourier Method

We can thus summarize the flexibility of the Fourier method of Sec.1.1 in deriving the expressions for the betatron frequencies-

- i) The equations are valid when the entry and exit spiral angles may be unequal.
- ii) The same expressions apply to conventional one magnet cyclotrons and separated sector cyclotrons. The latter are a special case with $B_V=0$.
- iii) For flat sectors $\eta_H = \eta_V = 0$. However, a field index in the bending magnets can be introduced through these terms.
- iv) By truncating the series at a low value of K, the "hard edge" expression (Eq.15) reduces to the correspondingly more accurate "soft edge" expression.

4. Optimum Sector Shapes

When optimizing the sector shapes for a separated sector cyclotron, it is required that the shapes be such that for some "reference ion", the time period be constant with the radius and simultaneously a prescribed tune be generated on the ν_r, ν_z graphs. If this is done, then eliminating ϵ_1 and ϵ_2 from Eqs.(5) and (15), the optimum contours for a separated sector cyclotron are given by simply^{1,2)}.

$$\Theta_1(\rho_0) = \int \frac{1}{2\rho_0} \left[R_1^2 \frac{2R_2}{R_3(S_1 - S_3)} \right]^{1/2} d\rho_0 - \frac{1}{2} \eta_0(\rho_0) \tag{19}$$

$$\Theta_2(\rho_0) = \Theta_1(\rho_0) + \eta_0(\rho_0) \tag{20}$$

where $R_1 = \rho_0 \frac{d\eta_0}{d\rho_0}$, $R_3 = \frac{1}{\pi^2} \left(\frac{BH}{B_0} \right)^2$, $K_1 = \frac{N\eta_0}{2\pi} \frac{BH}{B_0}$

$$R_2 = \left[S_1 R_3 R_1^2 + F^2 - K_1 n_H \frac{R_1}{R_4} - \nu_z^2(\rho_0) \right]$$

η_0 and $\frac{d\eta_0}{d\rho_0}$ are the prescribed sector angle and sector flaring required for isochronism and $\nu_z(\rho_0)$ the required radial variation of ν_z . The latter can be easily obtained from the tune to be generated^{1,2)}. In practice, $\frac{d\Theta_1}{d\rho_0}$ may be calculated at a few radii

in Eq.(19), fitted to a polynomial in radius, and integrated.

References

- 1) A. Jain and A.S. Divatia, IEEE Trans. Nucl.Sc. NS-20, No.3 (1973) p.902
- 2) A. Jain and A.S. Divatia, BARC Report 760, 1974
- 3) G. Schatz, Nucl.Instr. and Meth. 72 (1969) 29.
- 4) L. Smith and A.A. Garren, UCRL-8598(1959)
- 5) H.L. Hagedoorn and N.F.Verster, Nucl. Instr. and Meth. 18, 19 (1962) 201.

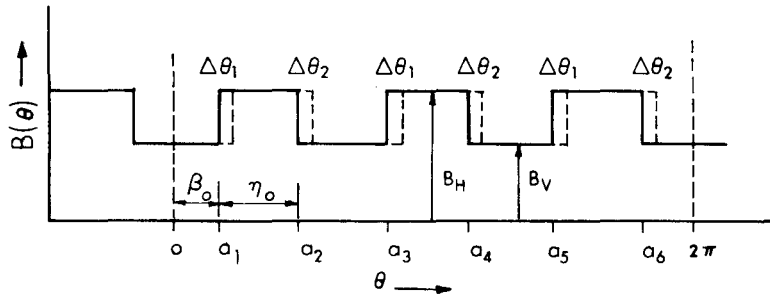


Fig.1 Step wave approximation for $B(\theta)$

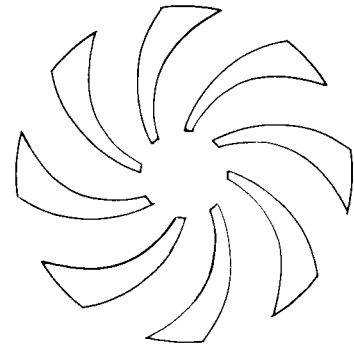


Fig.2 Sector shapes of an $N=8$, $E=1/3 mc^2$, separated sector electron cyclotron magnet.

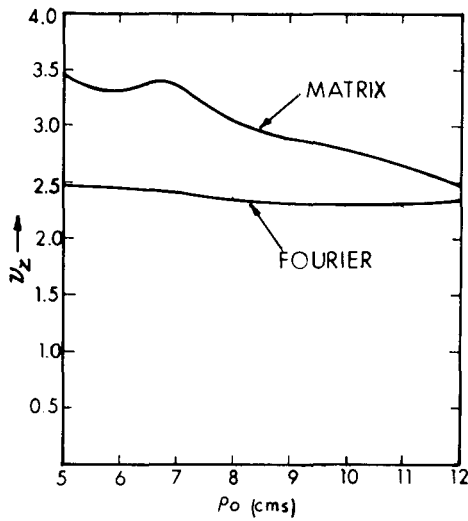


Fig.3 Comparison of ν_z obtained by using 1) the hard edge Fourier and ii) the matrix expressions for the same sector shapes, of Fig.2.

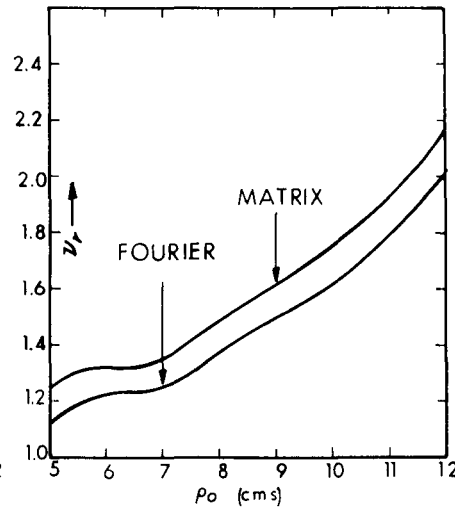


Fig.4 Comparison of ν_r obtained by using 1) the hard edge Fourier and ii) the matrix expressions for the same sector shapes, of Fig.2.

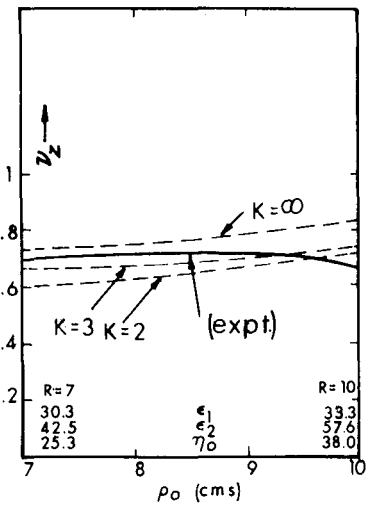


Fig.5 Comparison of soft edge Eq.(15) (with $K=2,3$) and hard edge Eq.(15)($K= \infty$) with orbit integration results in the measured field of an $N=3$ magnet.